Fish and Shellfish Immunology 91 (2019) 1–11

Contents lists available at ScienceDirect

Fish and Shellfish Immunology

journal homepage: www.elsevier.com/locate/fsi

Full length article

The key differentially expressed genes and proteins related to immune response in the spleen of pufferfish (*Takifugu obscurus*) infected by *Aeromonas hydrophila*

Shengli Fu[a,1], Mingmei Ding[b,1], Qingjian Liang[a], Yanjian Yang[a], Meng Chen[a], Xiufang Wei[a], Anli Wang[a], Shaoan Liao[a,**], Jianmin Ye[a,*]

[a] School of Life Sciences, South China Normal University, Guangzhou, 510631, PR China
[b] School of Medicine, Sun Yat-Sen University, Guangzhou, 510006, PR China

ARTICLE INFO

Keywords:
Takifugu obscurus
Aeromonas hydrophila
Spleen
IgT
Calcium signaling pathway

ABSTRACT

The immune mechanism elicited in pufferfish (*Takifugu obscurus*) against the invasion of *Aeromonas hydrophila* is still poorly understood. We examined the spleen of pufferfish at the transcriptome and proteome levels by using Illumina-seq and TMT coupled mass spectrometry after 12 h infection by *A. hydrophila*, respectively. A total of 2,339 genes (1,512 up-regulated and 827 down-regulated) and 537 (237 up-regulated and 300 down-regulated) proteins were identified. GO and KEGG analyses revealed that the responses to stimulus were the main biological processes, intestinal immune network for IgT production and calcium signaling pathway. Fourteen genes (8 up-regulated and 6 down-regulated) and proteins (5 up-regulated and 9 down-regulated) involved immune responses or signal transduction were validated by qRT-PCR and parallel reaction monitoring to confirm the reliability of the transcriptomic and proteomic analyses, respectively. Moreover, qRT-PCR and flow cytometry were used to detect dynamics of the genes in calcium signaling pathway and changes of concentration of cytoplasm Ca^{2+} in spleen cells within a 72 h challenge. This study provides the findings regarding immune response, especially intestinal immune network for IgT production pathway and calcium signaling pathway at the molecular, protein and cellular in pufferfish after infection by *A. hydrophila*. These results would provide a new insight and molecular targets into the response to pathogenic infection in pufferfish.

1. Introduction

Aeromona hydrophila, a well-known fish pathogenic bacterium, is widely distributed in aquatic environment [1]. It is known to produce a number of extracellular proteins, such as hemolysins, enterotoxins, proteases, lipases, chitinase, leucocidins, endotoxin, adhesions and so on [2], which are thought to be the causative agent of various symptoms including hemorrhagic septicemia, infection abdominal dropsy, bacterial hemorrhagic septicemia, epizootic ulcerative syndrome (EUS), hemorrhagic enteritis and red body disease [3]. In recent years, the aquaculture loses estimated to reach millions of dollars per annum due to *A. hydrophila* which attracted increasing attention of researchers [4]. It has been detected in a variety of fish species, including Nile tilapia (*Oreochromis niloticus*) [5], blunt snout bream (*Megalobrama amblycephala*) [6], common carp (*Cyprinus carpio*) [7], grass carp (*Ctenopharyngodon idella*) [8], zebrafish (*Danio rerio*) [9], and pufferfish (*Takifugu obscurus*) [10,11].

The teleost spleen is one of the major immune organs, which contains many immune cells, such as T and B cells [12], and is the major source of immunoglobulin. Meanwhile, it acts as a major secondary lymphoid organ to prevent further lesions during bacterial infections [13]. In addition, it has been reported that the teleost spleen can initiate the immune responses associated with calcium [14], and produce immune globulin to clean pathogens [15].

Up to now, an increasing number of studies about the teleost spleen in response to different stress, including pathogens, chemicals and

* Corresponding author. School of Life Sciences, South China Normal University, No.55 West Zhongshan Avenue, Guangzhou, Guangdong Province, 510631, PR China.
** Corresponding author.School of Life Sciences, South China Normal University, No.55 West Zhongshan Avenue, Guangzhou, Guangdong Province, 510631, PR China.
E-mail addresses: liaosha@scnu.edu.cn (S. Liao), jmye@m.scnu.edu.cn (J. Ye).
[1] These two authors contributed equally to this work.

https://doi.org/10.1016/j.fsi.2019.05.016
Received 15 February 2019; Received in revised form 7 May 2019; Accepted 8 May 2019
Available online 11 May 2019

temperature are analyzed by transcriptomics technologies [16–18]. The transcriptome analysis is fast and comprehensive, which has been constructed and annotated to aid in the identification of differentially expressed genes in distinct cell populations [19]. However, a comparison of mRNA expression levels is defined as indirect and temporarily messages in transmit information. On the contrary, proteins play a direct role in biological processes, and are the basis of organism [20]. Therefore, proteomic techniques have developed rapidly in recent years, especially isobaric tag for relative and absolute quantitation (TMT), which provide a lot of convenience for scientific research [21]. More and more studies in aquatic animals use TMT method to examine differentially expressed proteins, such as common carp (*Cyprinus carpio*) [4], Japanese flounder (*Paralichthys olivaceus*) [22], swimming crab (*Portunus trituberculatus*) [23], rainbow trout (*Oncorhynchus mykiss*) [24], grass carp (*Ctenopharyngodon idella*) [25], Atlantic salmon (*Salmo salar*) [26], and snakehead murrel (*Channa striatus*) [27]. These studies were focusing on the response to different stress, such as *A. hydrophila*, *Edwardsiella tarda*, *A. salmonicida*, fava bean intake and high temperature, in order to identify the different stress-responsive proteins.

The pufferfish, mainly distributed along the coastal regions of China, Japan and Korea, is an anadromous fish with high commercial value and attention in fish aquaculture [28]. Over the past few decades, a few of studies conducted in pufferfish had been reported at both molecular and physiological levels [29–31]. However, due to the lack of genomic sequence, the research progress of molecular mechanisms in pufferfish is slow. To our knowledge, this is the first time to combine transcriptomic and proteomic analyses to investigate the immune response in pufferfish. Here, we identified genes and proteins which were obtained from Illumina-seq and TMT searching for likely protein identification in NR, GO, KEGG, KOG, Swissport and Uniprot database, respectively, and focused on the differentially expressed genes (DEGs) and differentially expressed proteins (DEPs) in immune responses. GO and KEGG analysis were conducted among the DEGs and DEPs, revealing that response to stimulus was the main biological processes, intestinal immune network for IgT production and calcium signaling pathway were the mainly differential pathways activated. These results would provide a new insight and molecular targets into the systemic response to pathogens infection in teleost.

2. Materials and methods

2.1. Animals

Healthy pufferfish (*T. obscurus*) weighing 45.4 ± 5.2 g with a length of 13.2 ± 0.8 cm were purchase from an aquaculture farm in Panyu (Guangdong, China), and acclimated in 300 L cycling-filtered plastic tanks (6 fish/tank) for two weeks before the experimental treatments. During the acclimation period, the pufferfish were maintained in continuously circulating aerated water (pH 7.6 ± 0.2, temperature 25 ± 1 °C, ammonia nitrogen ≤ 0.05 mg/L, and dissolved oxygen ≥ 6.0 mg/L). The commercial fish diet (42% protein, 3.0% fat, 6.0% fiber and 16% ash, supplied by Dabeinong Group, Beijing, China) was employed to feed twice a day and no clinical sign of diseases was observed. All animal protocols were reviewed and approved by the University Animal Care and Use Committee of the South China Normal University.

2.2. Challenge and sample collection

The challenge experiment was performed by intraperitoneally injecting (100 fish per group) with 100 μL of *A. hydrophila* (BYK00810) (purchased from Key Laboratory of Exploration and Utilization of Aquatic Genetic Resources, Ministry of Eduction, P. R. China) suspension culture (1×10^8 CFU/mL) [32,33], which was cultivated in sterile Luria-Bertani Medium for 24 h at 28 °C, centrifuged at 5,000 rpm for 10 min at 4 °C [34] and then suspended in sterile phosphate buffer saline (PBS) as the treatment group. The fish injected with 100 μL sterilized PBS were used as the control group (100 fish per group). All fish were alive after the infection, but the pufferfish injected with *A.Hydrophia* showed slower activity, swimming irregular and hepatic hyperemia compared with the control group. Three fish from each group were anesthetized in 0.05% MS-222 (Tricaine methanesulfonare, Aladdin, Shanghai, China) and spleens were individually sampled for mRNA isolation and flow cytometry analysis at 0, 3, 6, 12, 24, 48 and 72 h post-challenge. In addition, three fish from each group were individually sampled at 12 h post-challenge [35,36], the highest percentage of spleen cells apoptosis time point (preliminary date), and immediately frozen in liquid nitrogen overnight and stored at −80 °C for RNA and protein extraction.

2.3. RNA isolation, library preparation, and sequencing

According to the RNA extraction protocols, total RNA was isolated by using Trizol reagent (Invitrogen, Waltham, MA, USA). The integrity and purity of the RNA were assessed by 1% agarose gels electrophoresis and the Nano Photometer® spectrophotometer (IMPLEN, USA), respectively. The quality and quantity of the RNA samples were determined by a Nanodrop2000 spectrophotometer (Thermo, USA).

Sequencing libraries were generated using NEBNext® Ultra™ RNA Library Prep Kitfor Illumina® (NEB, USA) following manufacturer's recommendations and index codes were added to attribute sequences to each sample. Briefly, mRNA was purified from total RNA using poly-T oligo-attached magnetic beads. Fragmentation was carried out using divalent cations under elevated temperature in NEBNext First Strand Synthesis Reaction Buffer (5 ×). First strand cDNA was synthesized using random hexamer primer and M-MuLV Reverse Transcriptase (RNase H-). Second strand cDNA synthesis was subsequently performed using DNA polymerase I and RNase H. Remaining overhangs were converted into blunt ends via exonuclease/polymerase activities. After adenylation of 3′ ends of DNA fragments, NEBNext Adaptor with hairpin loop structure were ligated to prepare for hybridization. In order to select cDNA fragments of preferentially 150–200 bp in length, the library fragments were purified with AMPure XP system (Beckman Coulter, USA). Then 3 μL USER Enzyme (NEB, USA) was used with size-selected, adaptor-ligated cDNA at 37 °C for 15 min followed by 5 min at 95 °C before PCR. Then PCR was performed with Phusion High-Fidelity DNA polymerase, Universal PCR primers and Index (X) Primer. At last, PCR products were purified (AMPure XP system) and library quality was assessed on the Agilent Bioanalyzer 2100 system. Then the library preparation was sequenced on an Illumina HiSeq platform and paired-end reads were generated. RSEM (version 1.2.15) was used to quantify the mRNA abundance [37].

2.4. Differential expression analysis for RNA-seq data

Expected number of fragments per kilobase of transcript sequence per millions base pairs sequenced (FPKM) values were obtained using Cufflink software (version 2.1.1), which was used as values for normalized gene expression [38]. Differential expression analyses of two comparison groups were performed using the DESeq R package (1.10.1) [39]. DESeq provide statistical routines for determining differential expression in digital gene expression data using a model based on the negative binomial distribution. The resulting *P*-values were adjusted using the Benjamini-Hochberg method [40]. Genes with an adjusted *P*-value < 0.05 and fold change > 2 found by DESeq were assigned as differentially expressed [41,42].

2.5. Protein isolation, enzymolysis, and TMT labeling

The spleen tissues were grinded by liquid nitrogen into cell powder in mortar and transferred to 4 mL lysis buffer (8 M urea, 1% Protease Inhibitor Cocktail) in a 5 mL centrifuge tube. After that, four volumes of

lysis buffer (8 M urea, 1% Protease Inhibitor Cocktail) were added to the cell powder, followed by sonication three times on ice using a high intensity ultrasonic processor (Scientz, China). The samples were centrifuged at 12,000 × *g* at 4 °C for 10 min and the debris was removed. Finally, the protein concentration was determined with BCA kit (Beyotime, China) according to the manufacturer's instructions.

For digestion, the protein solution was reduced with 5 mM dithiothreitol for 30 min at 56 °C and alkylated with 11 mM iodoacetamide for 15 min at room temperature in darkness. The protein sample was then diluted by adding 100 mM TEAB to urea concentration less than 2 M. Finally, trypsin was added at 1 : 50 trypsin-to-protein mass ratio for the first digestion overnight and 1 : 100 trypsin-to-protein mass ratio for a second 4 h-digestion.

After trypsin digestion, peptide was desalted by Strata X C18 SPE column (Phenomenex, USA) and vacuum-dried. Peptide was reconstituted in 0.5 M TEAB and processed according to the manufacturer's protocol for TMT kit. Briefly, one unit of TMT reagent was thawed and reconstituted in acetonitrile. The peptide mixtures were then incubated for 2 h at room temperature and desalted and dried by vacuum centrifugation.

2.6. LC-MS/MS analysis

The tryptic peptides were dissolved in 0.1% solvent A (formic acid), directly loaded onto a home-made reversed-phase analytical column (15-cm length, 75 μm i.d.). The gradient was comprised of an increase from 6% to 23% solvent B (0.1% formic acid in 98% acetonitrile) over 26 min, 23%–35% in 8 min and climbing to 80% in 3 min then holding at 80% for the last 3 min, all at a constant flow rate of 400 nL/min on an EASY-nLC 1000 UPLC system (Thermo, Waltham, USA).

The peptides were subjected to NSI source followed by tandem mass spectrometry (MS/MS) in Q Exactive™ Plus (Thermo) coupled online to the UPLC. The electrospray voltage applied was 2.0 kV. The *m/z* scan range was 350 to 1,800 for full scan, and intact peptides were detected in the Orbitrap at a resolution of 70,000. Peptides were then selected for MS/MS using NCE setting as 28 and the fragments were detected in the Orbitrap at a resolution of 17,500. A data-dependent procedure was alternated between one MS scan followed by 20 MS/MS scans with 15.0 s dynamic exclusion. Automatic gain control (AGC) was set at 5E4. Fixed first mass was set as 100 *m/z*.

2.7. Database search

The resulting MS/MS data were processed using Maxquant search engine (v.1.5.2.8). Tandem mass spectra were searched against Uniprot database concatenated with reverse decoy database. Trypsin/P was specified as cleavage enzyme allowing up to 2 missing cleavages. First search range was set to 5 ppm for precursor ions, and main search range set to 5 ppm and 0.02 Da for-fragment ions. Carbamidomethyl on Cys was specified as fixed modification and oxidation on Met was specified as variable modifications. FDR was adjusted to < 1% and minimum score for peptides was set > 40. Significantly changed proteins were identified using a Student's t-tests (a two-sided $P < 0.05$) and fold changes (> 1.2 or < 0.8333) [43,44].

2.8. Confirmation using qRT-PCR and PRM-MS analyses

To validate the veracity transcriptome result, fourteen DEGs involved in immune responses were selected for validation using qRT-PCR. The RNA used for qRT-PCR were the same with those used to construct cDNA library. The primers were designed using Primer 5.0 (Table 4) and synthesized by Tsingke Biological Technology Co., Ltd and *β*-actin (GenBank Accession NO. EU871643.1) acted as the reference gene. The qRT-PCR with SYBR Green dye (TaKaRa, Japan) was performed on an ABI 7500 Real-Time PCR system (Applied Biosystem, USA) [45]. The qRT-PCR reaction volume was 20 μL, containing 3 μL of 1:10 diluted cDNA, 10 μL of 2 × TaKaRa Ex Taq™ SYBR premix, 2 μL of each primer (10 μM), 0.4 μL ROX Reference Dye II (Takara, Japan) and 2.6 μL ddH_2O. The PCR program was 94 °C for 30 s, followed by 40 cycles at 95 °C for 5 s, 60 °C for 30 s and 1 cycle of 95 °C for 30 s, 60 °C for 60 s. The melting curve analysis was implemented to confirm the credibility of each qRT-PCR analysis. Each sample was analyzed in triplicate to certify the repetitiveness and credibility of experimental results was measured by using 7500 SDS software (Applied Biosystem, USA) with $2^{-\Delta\Delta Ct}$ methods [46] and one way analysis.

To confirm the protein expression levels obtained using TMT analysis, the PRM-MS analysis carried out at the Jingjie PTM BIO (Hangzhou, China) Co., Ltd. The proteins (60 μg) used for PRN-MS analysis were the same with the TMT analysis and were prepared, reduced, alkylated, and digested with trypsin following the protocol for TMT analysis. The obtained peptide mixtures were dissolved in 0.1% solvent A, directly loaded onto a home-made reversed-phase analytical column (15 cm length, 75 μm i.d.). The peptides were subjected to NSI source followed by tandem mass spectrometry (MS/MS) in Q Exactive™ Plus (Thermo, USA) coupled online to the UPLC. Fourteen proteins were selected, including five up-regulated and nine down-regulated.

2.9. Cytoplasmic free-Ca^{2+} concentration in spleen cells

The cell-permeant probe Fluo-3/acetoxymethyl ester (fluo-3/AM) (Beyotime Biotechnologies, China) was used to monitor the level of intracellular calcium concentration, as described by a previous method [47]. In brief, the spleen tissue from each of fish was collected and washed by RPMI-1640 (Gibco, USA) to remove blood and fat cells, broken lightly and filtered with 200 mesh screen (BD, USA), then the number of cells were calculated and the cell concentration was adjusted to 0.5×10^7 cells/mL. Diluted spleen cells 200 μL was obtained and then incubated with 10 μM fluo-3/AM for 30 min in the dark, washed three times by sterile PBS and suspended by 200 μL PBS. To detected the green fluorescence emitted by fluo-3/AM de-esterified with cytoplasmic free calcium, the flow cytometry (BD) was set up ($\lambda_{excitation} = 506$, $\lambda_{emission} = 526$). Cytoplasmic free-Ca^{2+} concentration was expressed as mean fluorescence of fluo-3/AM.

3. Results

3.1. Overview of RNA transcriptome and proteome profiles of pufferfish spleen

A total of 167,946 transcripts and 101,455 genes, with an average length of 1,154 bp and 1,716 bp (ranging from 201 bp to 24,814 bp) and an N_{50} of 2,642 bp and 2,986 bp were resulted by the transcriptome sequencing. The statistics of the sequencing data and the assembly results were summarized in Table 1. To assess the quality of the

Table 1
Summary of the transcriptome and proteome data in the spleen of pufferfish.

Transcriptome date		Proteome date	
Output results		MS/MS spetrum database	
Raw reads (mean)	52,429,761	Total spectrums	188,618
Clean reads (mean)	50,510,712	Peptides	21,588
GC percentage (mean)	50.31%	Unique peptides	20,550
High quality reads		Quantifiable proteins	3,672
Q20 (mean)	97%		
Q30 (mean)	92.5%		
Assembly results			
Transcripts number	167,946		
Total Nucleotides (bp)	193,786,149		
Transcripts N50 length (bp)	2,642		
Transcript mean length (bp)	1,154		
Transcript largest length (bp)	24,814		
GC percentage (%)	50.63		

transcriptome, the unigene at Supplementary Fig. 1A showed the distribution of raw read lengths, a decreasing number of transcripts with increasing unigene length. In order to obtain comprehensive genetic information, we carried out the genetic function notes of seven databases (Nr, Nt, KO, SwissProt, Pfam, KOG/COG, GO), all of the 101,455 genes were annotated, of which 21,948 genes were found in a Venn diagram of pufferfish spleen in five databases (Supplementary Fig. 1B). By comparing and annotating with the Nr database, 54,577 (53.79%) showed positive hits. The spleen transcriptome of pufferfish and tiger puffer (*Takifugu rubripes*, 74.3%) had the highest similarity, followed by croceine croaker (*Larimichthys crocea*, 7.3%) (Supplementary Fig. 1C). In addition, other fishes such as bicolor damselfish (*Stegastes partitus*, 3.2%), Nile tilapia (*Oreochromis niloticus*, 2%), and tongue sole (*Cynoglossus semilaevis*, 0.8%) were also in the top of the top. Then, the RNA-Seq reads mapped to the databases were aligned and estimated. In total, 87,961 expressed genes were detected in the spleen tissue examined and 2,339 DEGs (1,512 up-regulated and 827 down-regulated) were detected in the comparisons of experimental and control group (Supplementary Fig. 2A) (Supplementary Table 1).

In addition, by searching against the pufferfish Uniprot database, 4,133 proteins were identified from a total of 188,618 spectra, 21,588 peptides, and 20,550 unique peptides in the proteomic analysis. A total of 537 DEPs (237 up-regulated and 300 down-regulated) have showed significantly differential expression (Supplementary Fig. 2B) (Supplementary Table 2).

3.2. GO and KEGG enrichment analysis of DEGs and DEPs

In biology, different genes coordinate and exercise their biological functions, so the most important biochemical pathways and signal transduction pathways of gene participation are determined by the significance enrichment of pathway. GO functional annotations were used to better understand the biological functions of DEGs and DEPs in pufferfish. All the genes and proteins were classified into three categories: biological process, cellular component, and molecular function. The significant GO terms in these three categories and DEGs and DEPs of them were showed in Fig. 1A and B. For the DEGs, we found that 3,265 GO terms were assigned to 2,339 transcripts, including 2,313 and 2,913 terms for up and down-regulated genes, respectively (Fig. 1A and B). For the 537 DEPs, 237 up-regulated proteins were annotated to 104 GO terms, whereas 300 down-regulated proteins were assigned to 142 GO terms.

KEGG analysis was performed and all the DEGs and DEPs were assigned. Among 2,339 DEGs and 537 DEPs resulting from the comparison between experimental versus control group, 1,062 genes could be annotated to 282 KEGG pathways and 199 proteins were annotated to 30 KEGG. Basically, the main 6 KEGG pathways were classified: i) organismal systems; ii) human diseases; iii) metabolism; iv) environmental information processing; v) genetic information processing; and vi) cellular processes. Platelet activation, calcium signaling pathway, Fc gamma R-mediated phagocytosim, chemokine signaling pathway, B cell receptor signaling pathway, T cell receptor signaling pathway, Toll-like receptor signaling pathway and Intextinal immune network for IgT production were the important terms of DEGs associated with immune responses. Calcium signaling pathway, cell adhesion molecules (CAMs) and Intestinal immune network for IgT production were the important terms associated of DEPs with immune responses.

To detect whether DEPs were significantly enriched in some functional types, we performed enrichment analysis of functional annotation type of KEGG, as seen in Fig. 2A and B. The up-regulated proteins were mainly annotated to metabolic pathway, and the down-regulated to immune related pathways and signal transduction, such as intestinal immune network for IgT, calcium signaling pathway and so on. There were three down-regulated proteins between experiment and control group in intestinal immune network for IgT production (https://www.kegg.jp/kegg-bin/show_pathway?map04672) (Fig. 2C). In calcium signaling pathway, we found two up-regulated proteins and seven down-regulated proteins (https://www.kegg.jp/kegg-bin/show_pathway?map04020) (Fig. 2D).

3.3. Analysis of DEGs and DEPs related to immune responses

In this report, we focused on the genes and proteins related to the immune responses. Differential expression genes and proteins involved in both innate and adaptive immunity had been identified, including 48 up-regulated and 42 down-regulated genes and 3 up-regulated and 7 down-regulated proteins (Supplementary Table 3) (Supplementary Table 4). The genes were grouped into 16 sub-classes and the main pathways as follows: Intestinal immune network for IgT production, Chemokin signaling pathway, antigen processing and presentation, B cell receptor signaling pathway and so on and the proteins were grouped into Intestinal immune network for IgT production and calcium signaling pathway.

3.4. Correlation analysis of RNA and protein expressions

To investigate the correlation of expression level in mRNA and protein, the DEPs obtained in pufferfish spleen proteome analysis were compared with the mRNAs corresponding to transcriptome analysis. The results shown 29 proteins (5.4%) differentially expressed at both mRNA and protein levels between experimental and control groups as seen in Supplementary Table 5. Among these, 25 genes were changed in the same direction (either up or down) (Table 2) at the transcriptional and translation levels, indicating that only partial correlations were found at the mRNA and protein levels of overall gene expression.

3.5. Analysis of DEGs and DEPs by qRT-PCR and PRM

Quantitative real-time RT-PCR and PRM were performed on some selected targets in both experimental and control groups to provide additional mRNA transcript levels and validate the proteome results. Fourteen immune related genes, including eight up-regulated and six down-regulated were detected. As shown that the mRNA expression levels of *CD276*, *HERC1*, *HCRC1*, *CAMK2*, *SDC2*, *ATP2B*, *ITGA4* and *CDH5* was significantly up-regulated at 12 h post-infection (dpi) compared to that of the control group (Fig. 3). On the other hand, Fig. 3 showed that the mRNA expression of *RASGRP2*, *STX7*, *SUN1/2*, *MHC II*, *CHRNA7* and *ZMYM4* was significantly down-regulated after infection. There results indicated that transcriptome results indeed reflected the relative expression level of each gene *in vivo*, in which up-regulated or down-regulated genes in qRT-PCR were completely consistent with the results of transcriptome.

At the same time, fourteen DEPs (up-regulated: ITGB1, PVRL1, MRC, RAC1 and MAO; down-regulated: IGH, CD38, MHC II, CDH1, MHC I, COL1A, CTSL, TFRC and ATPeV0A) were selected for the PRM analysis. They were responsible for immune responses or signal transduction. The expression values and fold changes for these proteins were significantly different between the experimental and control groups, in agreement with the findings of the TMT analysis (Table 3).

3.6. Assessing calcium activity and related genes expression post-challenge in pufferfish spleen

Finally, we experimentally confirmed the alterations of calcium activity by injection with *A. hydrophila*. As shown in Fig. 4A, the concentration of cytoplasmic free-Ca^{2+} were significant increased at 12 h and 24 h ($p < 0.05$) after challenged, then began to decrease until 72 h.

The expression patterns of *SERCA* and *CD38* were investigated at 0, 3, 6, 12, 24, 48 and 72 h following *A. hydrophila* challenge in spleen. Both of them were DEPs in calcium signaling pathway. As seen in Fig. 4B, the basal transcript level of *SERCA* was elevated at the early

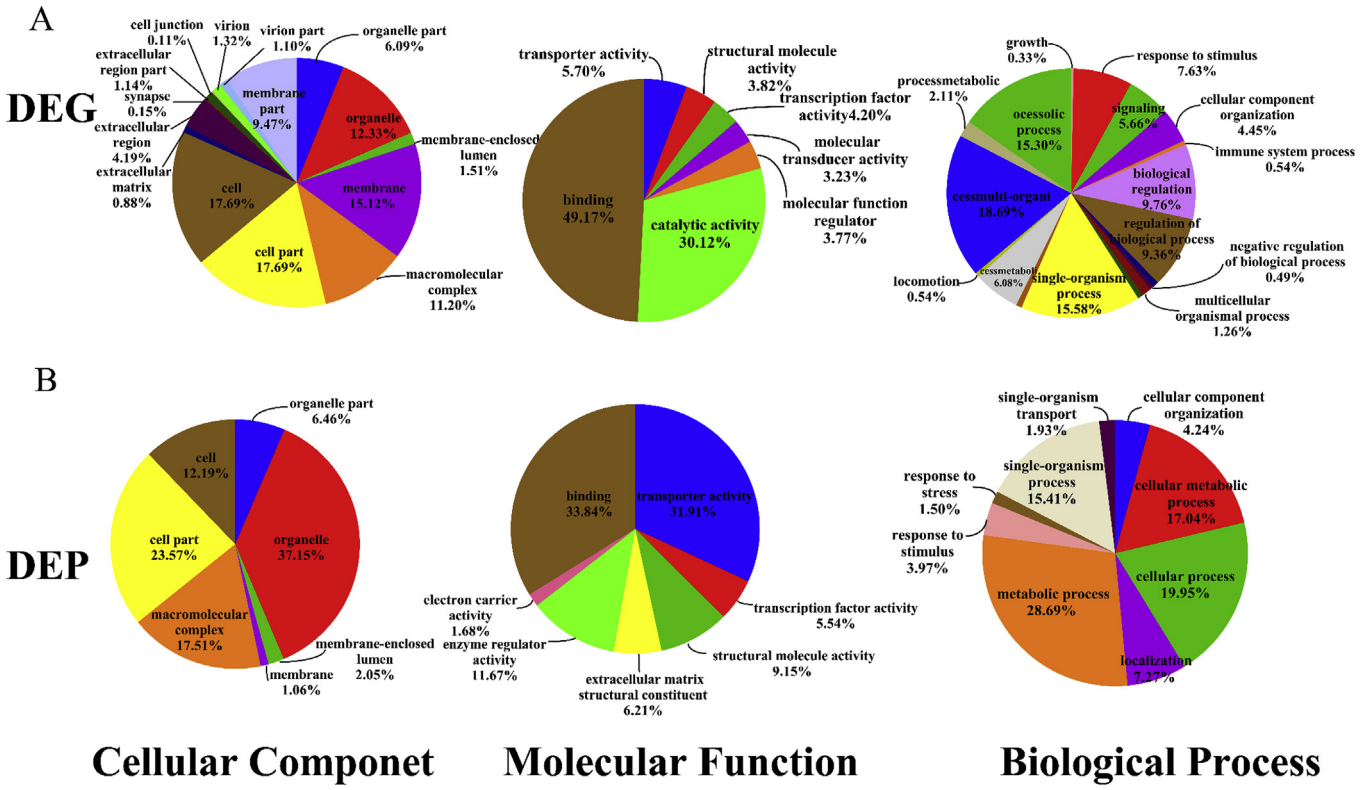

Fig. 1. GO categories assigned to the significantly up-regulated (A) and down-regulated (B) transcripts (DEG) and proteins (DEP) in pufferfish spleen in response to *A. hydrophila*. The genes and proteins were categorized on the basis of GO annotation. The proportion of each category displayed is based on cellular component, molecular function and biological process in percentage. Left, transcripts (DEG) and right, proteins (DEP).

phase (3 h post-treatment), and then down-regulated until 24 h post-infection. It also significantly increased at 48 h post-infection ($p < 0.05$), and then went down to the initial state at 72 h. The *CD38* gene expression was down-regulated until 24 h post-treatment and significantly increased at 48 h post-infection and then went down to the initial state at 72 h.

These data collectively in Fig. 4 not only validated DEGs and DEPs, but also confirmed in particular the down-regulation of cellular pathways related to immune responses or calcium signaling pathway shown in the network model.

4. Discussion

With the recent advancement of DNA sequencing technology, more and more studies about the molecular mechanisms mediate the immune response of fishes against pathogen infection [48,49]. In this study, there were a total of 2,339 DEGs and 537 DEPs between experimental group and control group, which were assigned multiple potential function in molecular function and biological process. The number of the same direction (either up or down at transcription level and protein level) identified genes was 25, indicating that only partial correlations were found at the mRNA and protein levels of all genes expression, which may be caused by post-transcriptional regulation and post-translational modifications or other unknown factors [50]. GO and KEGG analyses suggested that immune system and the signal transduction were the differential pathways activated at transcription level and protein level, 16 immune-related categories involving 90 DEGs were scrutinized. Especially intestinal immune network for IgT production and calcium signaling pathway.

4.1. Consistently expressed genes at RNA and protein levels

Only nine of the proteins, Syntaxin-7 (STX7), Poly [ADP-ribose] polymerase 3 (PARP), Tyrosine-protein kinase HCK (HCK), Cytidine deaminase-like (CDA), L-lactate dehydrogenase A chain (LDH), Keratin (KRT1), Thrombomodulin (THBD), G6P aminotransferase [isomerizing] 2 (GFPT), gamma-glutamyl hydrolase-like (GGH), whose RNA and protein levels were consistent were annotated into KEGG pathway. Most of them were metabolism-related enzymes, such as CDA, LDH, GFPT, GGH, there were up-regulated, which indicated that the metabolism might be activated in pufferfish spleen tissues after infected with *A. hydrophila*. HCK is a member of the SRC family of cytoplasmic tyrosine kinases, it can enhance immune and epithelial cell invasion [51], its up-regulation might be the result of pathogen infection. KRT1 is a member of keratin family and its constitution and expression patterns are complex and often distinctive in human [52]. THBD serves as a cofactor for thrombin, it can enhance the specificity of the latter serine protease and increase their proteolytic activation rate with concomitant anticoagulant, antifibrinolytic and anti-inflammatory benefits to the vascular wall [53]. STX7 is contained in endosomes and is importance in the early phases of endo-phagocytic pathway [54], PARP is a family of proteins involved in a number of cellular processes such as DNA repair, genomic stability and programmed cell death [55]. Both of them were down-regulated, which were consistent with the down-regulated result that the apoptosis of spleen cells reached the peak after 12 h of infection with *A. hydrophila*.

4.2. Intestinal immune network for IgT

In the intestinal immune network for IgT production pathway, the major histocompatibility complex II (MHC II) recognizes and presents antigens to the B-cell activating factor (BAFF), interacting with the transmembrane activator and CAML interactor (TACI) and ultimately resulting in B cell differentiation into IgT^+ B cells [56,57]. It is known that the IgT antibodies are produced by IgT^+ B cells and a major functional component of humoral branch of the adaptive immune

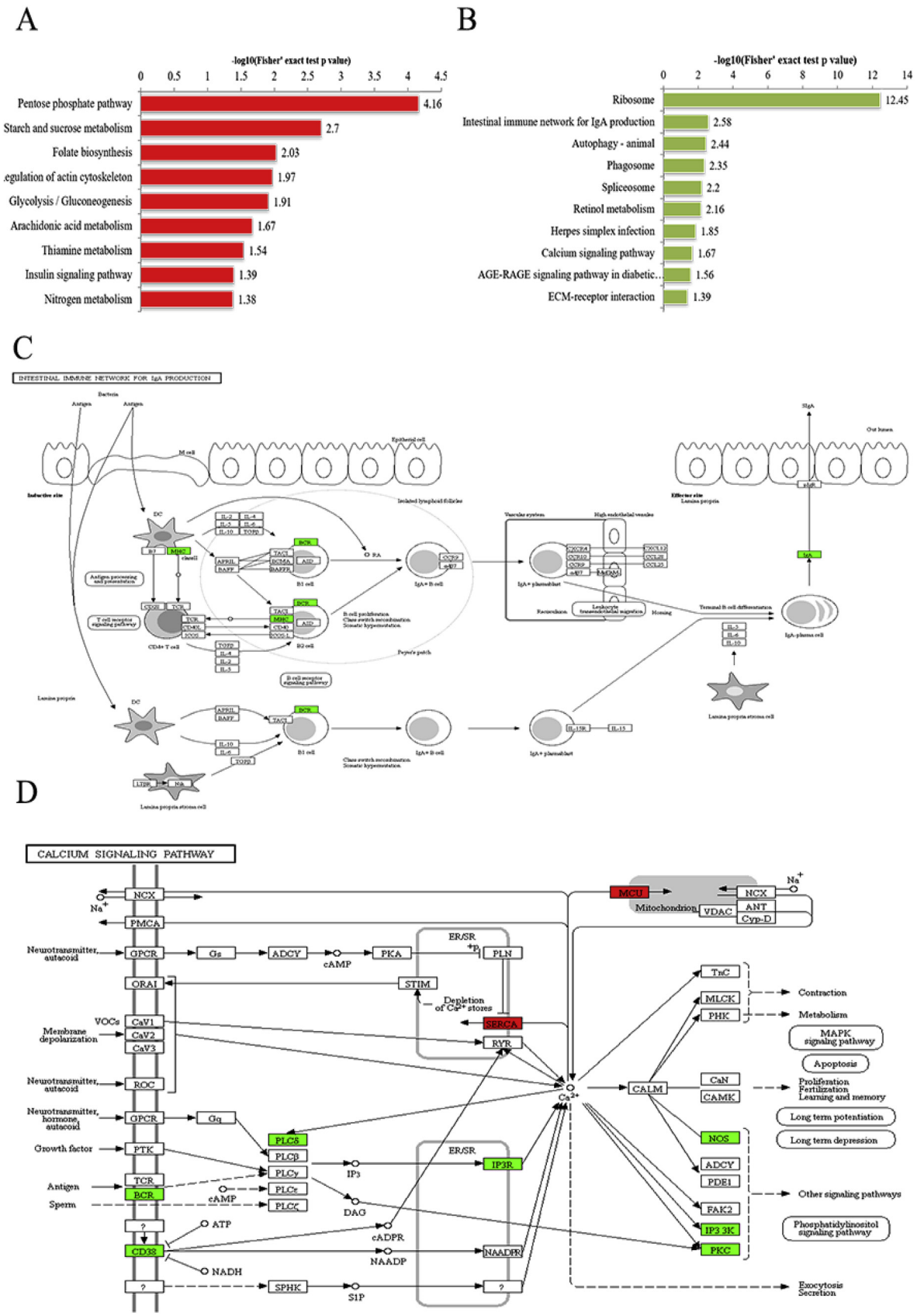

Fig. 2. The enrichment analysis of functional annotation type of KEGG from pufferfish spleen in response to *A. hydrophila*. (A) The top terms of proteins KEGG for the up-regulated DEPs. (B) The top terms of KEGG pathway for the down-regulated DEPs. (C) and (D) were visual representations of significantly enriched intestinal immune network for IgT production pathway and calcium signaling pathway of differentially expressed proteins. Negative logarithms (-log10) of the *P*-values obtained for the enrichment test (Fisher's exact test here) result in a more significant enrichment of this type of function as the converted value gets larger. Red means up-regulated protein in KEGG pathway, and bright-green means down-regulated protein in KEGG pathway. (For interpretation of the references to color in this figure legend, the reader is referred to the Web version of this article.)

Table 2
The consistent expression proteins at RNA and protein levels.

Uniprot accession number	Unique peptides	Protein length	MW [kDa]	Fold change in proteins	p-Value (proteins)	Gene id	Counting Length	Log2 fold change in contigs	p-Value (contigs)	Protein description
Up-regulated proteins										
O35086	8	336	36.9	1.689	1.25E-08	Cluster-6421.14135	1138	2.8474	8.66E-03	Haptoglobin-like isoform X2
P27216	6	352	39.4	1.445	2.80E-09	Cluster-6421.38542	2074	1.725	4.39E-02	Annexin A 13-like isoform X3
S9XJZ0	5	468	53.3	1.721	4.21E-04	Cluster-6421.39699	2383	3.2668	1.04E-06	Plasmalemma vesicle-associated protein-like
Q95M30	10	498	56.1	1.292	1.54E-05	Cluster-6421.40198	2189	2.1682	2.59E-03	Tyrosine-protein kinase HCK
P56389	5	166	18.2	1.261	3.99E-02	Cluster-6421.41974	933	1.8267	3.02E-02	Cytidine deaminase-like
Q80V70	5	1616	172	1.672	4.22E-07	Cluster-6421.42558	11381	1.8444	2.06E-02	Growth factor-like domains protein 6
Q92055	11	361	39.5	1.201	3.79E-08	Cluster-6421.42728	1230	3.1328	3.05E-06	L-lactate dehydrogenase A chain
P43121	8	644	70.9	1.298	3.11E-10	Cluster-6421.42745	2153	2.1556	1.01E-02	Cell surface glycoprotein MUC18
Q0VCM6	2	602	66.3	1.392	5.52E-03	Cluster-6421.42789	2543	2.0809	6.42E-03	Large neutral amino acids transporter small subunit 4-like
P17213	14	504	55.4	2.16	1.00E-32	Cluster-6421.42838	1906	3.1224	2.92E-06	Bactericidal permeability-increasing protein-like
O57607	34	464	51.5	1.213	1.00E-32	Cluster-6421.42844	1842	1.8841	1.80E-02	Keratin
P15306	3	553	60.1	1.273	8.84E-03	Cluster-6421.43058	2861	2.1743	4.15E-03	Thrombomodulin
Q687X5	9	528	58.4	1.766	5.00E-15	Cluster-6421.43079	2254	2.6892	1.09E-04	Metalloreductase STEAP4
Q4KMC4	19	687	76.8	1.369	1.00E-32	Cluster-6421.43478	3264	2.6772	1.12E-04	G6P aminotransferase [isomerizing] 2
Q96RW7	44	5536	597	1.256	1.00E-32	Cluster-6421.43775	17325	3.8646	4.70E-09	Hemicentin-1
Q9NZN3	3	551	62.2	1.407	7.50E-03	Cluster-6421.46329	2753	2.0412	1.48E-02	EH domain-containing protein 3
Q14108	5	547	61.7	1.458	2.70E-06	Cluster-6421.46716	2864	1.7543	4.10E-02	Lysosome membrane protein 2-like isoform XI
Q92820	3	328	36.5	3.319	1.47E-02	Cluster-6421.46871	1534	2.8006	4.52E-05	Gamma-glutamyl hydrolase-like
P35555	17	466	49.1	1.485	6.66E-16	Cluster-6421.48613	1784	3.8345	4.95E-05	Fibrillin-1
Q9NQT8	3	1840	205	1.213	4.14E-03	Cluster-6421.52329	9891	2.4622	9.86E-04	Kinesin-like protein KIF13B isoform X2
Q8CGB3	14	1395	158	1.332	5.91E-05	Cluster-6421.56258	6357	2.3891	5.34E-13	Uveal autoantigen with coiled-coil
Down-regulated proteins										
Q3ZBT5	3	241	26.8	0.596	7.60E-03	Cluster-6421.24897	3018	−2.1631	1.70E-02	Syntaxin-7
Q9Y6F1	8	523	58.8	0.692	5.30E-03	Cluster-6421.27941	3163	−3.4192	1.10E-03	Poly [ADP-ribose] polymerase 3
O13089	2	294	32.4	0.781	7.38E-03	Cluster-6421.52408	4224	−2.9386	2.36E-03	DNA-binding protein Ikaros isoform XI
O35130	2	244	26.8	0.771	7.42E-03	Cluster-6421.71387	2996	−2.7906	1.09E-05	kell blood group glycoprotein isoform X1

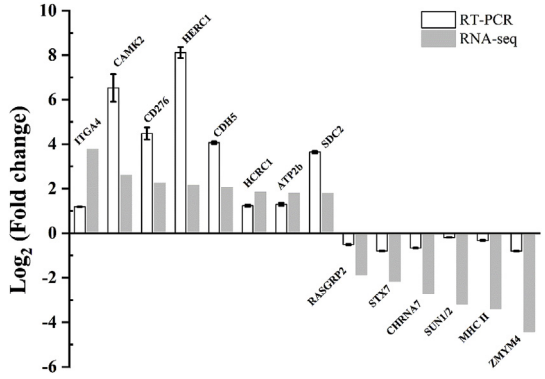

Fig. 3. Comparison of the expressions of RNA-Seq and qRT-PCR results. The transcript levels of the selected genes were each normalized to that of the *β*-actin gene. The relative expression of the transcript from qRT-PCR was calculated based on the standard curve and normalized to the *β*-actin gene. The calculated data (mean ± SEM) of three individual ($n = 3$).

Table 3
Confirmation of DEPs detected in TMT analysis using PRM analysis.

Accession	Gene Symbol	Fold change (SY/DZ) in TMT	Fold change (SY/DZ) in PRM
Cluster-6421.40274_1	IGH	0.811	0.51
Cluster-6421.42251_2	CD38	0.665	0.35
Cluster-6421.41954_1	MHC2	0.081	0.62
Cluster-6421.48361_1	CDH1	0.657	0.48
Cluster-6421.44159_1	MHC1	0.762	0.52
Cluster-6421.42167_1	ITGB1	1.363	1.15
Cluster-6421.37122_1	PVRL1	1.215	1.06
Cluster-6421.43311_1	COL1A	0.421	0.28
Cluster-6421.50922_1	CTSL	0.779	0.65
Cluster-6421.43469_1	TFRC	0.779	0.68
Cluster-6421.43237_1	ATPeV0A	0.755	0.49
Cluster-6421.43048_1	MRC	1.262	1.26
Cluster-6421.27810_1	RAC1	1.23	1.12
Cluster-6421.59442_1	MAO	1.419	1.35

system [58], it can function in high-affinity modes for neutralization of toxins and pathogenic microbes [58]. Further, MHC II, a cell surface protein, is a key player in initiating immune response towards invading pathogens [59]. One previous report indicated that the expression of *MHC II* in blunt snout bream (*Megalobrama amblycephala*) was higher in immune related tissues and increased within 72 h after *A. hydrophila* infection in gill and kidney [60]. Differently, in our study, *MHC II* was significantly decreased in the expression at transcript and protein levels within 12 h after infection of *A. hydrophila*. It was verified by qRT-PCR in Fig. 3 and PRM in Table 3, respectively. Interestingly, it was similar to the studies in half-smooth tongue sole (*Cynoglossus semilaevis*) and turbot (*Scophthalmus maximus*) [61,62]. These results suggested that the same genes expressed in different tissues or stimulated by different pathogens may have different expression patterns. Another possibility is that crucial interference of cellular function occurs under a semilethal concentration of pathogenic bacteria in immune tissues. After injection, the pathogens first added value in the body, the cellular function of immunity organs may be destroyed and the corresponding expression may decrease [62]. Further studies will be needed for elucidating the precise role and mechanism of MHC genes in defense response in fish.

In human, IgA is present in serum (peripheral blood) and mucosal juice (mucosal tissues), which displays a unique heterogeneity in its molecular forms and in various degrees of aggregation [63]. Until now, there has been found three main types of immunoglobulins (Igs) in teleost: IgM, IgD, and IgT/IgZ [64]. The IgT/IgZ was first discovered in rainbow trout and zebrafish in 2005 [65,66], respectively, and analogous to mammalian IgA [67]. The expression and distribution patterns of IgT have certain tissue specificity with relative high expression in mucosal tissues, but still exhibit considerable variation in different fish species [68]. Until now, there are no studies on immunoglobulins in pufferfish. In this study, the IgT in pufferfish spleen was down-regulated at protein level at 12 h post-infection after *A. hydrophila* challenge and no significant change at transcriptional level. One possibility is that, similar to the mechanics for the expression pattern of *MHC II* molecule upon challenge, the IgT was down-regulated at 12 h dpi. Another possibility is that the predominant Ig isotype was IgM which was amplified after *A. hydrophila* infection [69] to clear the pathogen, since the spleen tissue is one of main organs to produce IgM, not the IgT [70,71]. The expression and distribution patterns of IgT in pufferfish remains to be further studied.

4.3. Calcium signaling pathway

Calcium signal controls majority of cellular reactions. Further, it is essential for diverse cellular functions including differentiation, effector function, and gene transcription in the immune system [72]. Calcium ions (Ca^{2+}) can function as a second messenger in different cells of the immune system, particularly in B and T lymphocytes, macrophages and mastocytes [73]. There are several factors that can increase the concentration of Ca^{2+}, mainly including intracellular IP3 and IP3 receptor binding, or cyclic ADP-ribose (cADPR) combination with RyR, opening the endoplasmic reticulum (ER) Ca^{2+} channel, releasing the ER Ca^{2+} into the cytoplasm, and extracellular Ca^{2+} entering the cytoplasm through voltage operated calcium channel (VOC), receptor operated

Table 4
Primers used for qRT-PCR verification of differently expressed genes.

Gene	Forward primer (5′-3′)	Reverse primer (5′-3′)
STX7	CGGGAGGACAACCAGAAGACA	CAGACTCTAACTGCCTGATGGATAA
RASGRP2	CAAGAGCATCAGCCACGAGG	GCAGGCTGGGCAAGGTGTT
CD276	TTTGCGTCCAGGCGATGAA	TCCAGCACAACCGTGAGCA
SUN1/2	GAAAATGTGCGTCAAAAAACCG	TCGTCTTCATCCGTCTGTCTGTA
CAMK2	TCCTCCGACAGCAGCAACAC	CGAATGAGGTCAAGCCAGGA
SDC2	GCTGTTGTTTCTCGTGGGGC	AGTTGCCTGAAGTTCTGCCCTC
ITGA4	TGGTGTTCAGTGGTCCTCCG	CACAACTGTAAATGGCTCCCG
CDH5	ACAATGGGGCTCCTGGCTG	GCGACTGGTGCTGGTTTCTC
ATP2b	CTGTGGAAGGGCTGCTGGC	TTGAATGACCTGCCCTCCG
MHC II	ACGGAGTCTACGGCACCCC	TGGGAGCAACTGTCTCTGGC
CHRNA7	GCTGGGGGTCCTGGCGTA	CTCCCTGCGATGGAAAGACA
HERC1	TGAATGCGAGTCCAGTGCCT	GGTATTTGCTGTGGATTGCGTA
HCFC1	AAGGCAAGCAGGAAATCACG	TGATAGTGGTGGCAGAGTGAAGAC
ZMYM4	CCTCCAGGGGCTCTGTAACC	AGCACCTCTCCAGACCCTTCC
CD38	TTGAGCAAGCGTATGTGGGG	GGACCACATCCTTCGTTTTGC
SERCA	CCGTGATGAGATGGCTGCTAC	TGGACGGGGTCGTTGAAGT
β-actin	CATCACCATCGGCAACGAGAGG	CGTCGCACTTCATGATGCTGTTG

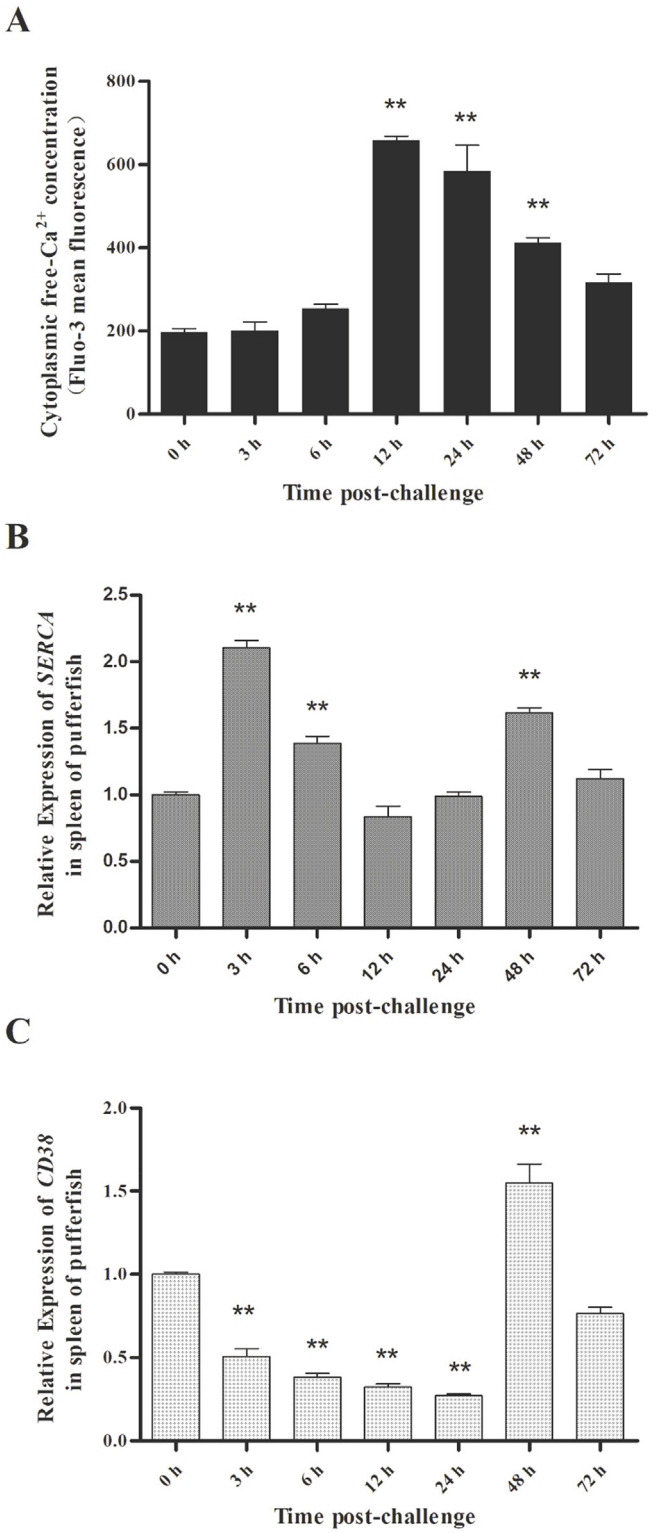

Fig. 4. Cytoplasmic free-Ca^{2+} concentration (A) and relative expression levels of *SERCA* (B) and *CD38* (C) at 0, 3, 6, 12, 24, 48, and 72 h after *A. hydrophila* challenge. Control samples were injected with PBS. The relative expression of the transcript from qRT-PCR was calculated based on the standard curve and normalized to the *β*-actin gene. The results are shown as mean ± SEM ($n = 3$) and Significant differences was indicated by asterisk (*: $0.01 < p < 0.05$, **: $p < 0.01$).

calcium channel (ROC) and store operated calcium channel (SOC) [73]. To reduce the cytoplasmic Ca^{2+} mainly rely on different calcium pumps, such as sarcoplasmic reticulum Ca^{2+}-ATPase (SERCA) [74,75].

In mammals, the maintenance of Ca^{2+} homeostasis is important. They are not metabolized by the cell, instead, they enter into the cell cross either the ion channels on plasma membrane or the store-operated calcium channel on the membrane of intracellular organelles [76]. Once they enter the cytosol of the cytoplasm, they exert allosteric regulatory effects on many enzymes and proteins [77]. Whether regulation of Ca^{2+} and the activation of calcium signal pathway by Ca^{2+} in fish similar to that in mammals or not needs to be further studied. This is the first study of calcium signaling in pufferfish from the transcriptional and protein levels. In our results, the nicotinic acetylcholine receptor alpha-7 (*CHRNA7*), a non-selective cation channel [78], was down-regulated in transcriptional. In contrast, the plasma membrane Ca^{2+} ATPase (*PMCA*), a transport protein in the plasma membrane of cells and functions to remove Ca^{2+} from the cells [79], was up-regulated. These two genes were involved in the entry of Ca^{2+} into the cytoplasm [80,81] and verified by qRT-PCR in Fig. 3. PMCA has been studied in zebrafish (*Danio rerio*) and tilapia (*Oreochromis mossambicus*) [82,83]; however, there is still no comprehensive studies published on the role of PMCA in Ca^{2+} regulation, or molecular evidence of its expression. Myosin light chain kinase (*MYLK*), calmodulin dependent protein kinase II (*CAMK2*) and classical protein kinase C alpha type (*PRKCA*) were significantly up-regulated in transcriptional. These kinases were calcium dependent [84–86] and their transcriptional levels were consistent with changes in cytoplasmic Ca^{2+} concentration (Fig. 4A). Until now, studies related with these three genes have not been reported in teleost. In human, Ca^{2+} in the cytoplasm binds to calmodulin, which in turn changes the conformation of protein kinase and thus regulates the metabolic process. MYLK participates in inflammation and migration [87]; CAMK2 could mediate the expression bone associated proteins and improve osteoblast differentiation [88] and PRKCA was required for, and modulate keratinocyte differentiation in opposing directions [86].

SERCA, a Ca^{2+} ATPase transfers Ca^{2+} from the cytosol of the cell to the lumen of SR [74], was up-regulated at protein level. And CD38 was down-regulated, which is a multifunctional ectoenzyme and essential for the regulation of intracellular Ca^{2+} [89]. However, both of them had no significant changes at transcriptional level. Their expressions were also verified by PRM analysis. In addition, we detected the expressions of *SERCA* and *CD38* in pufferfish spleen after *A. hydrophila* challenge at 0, 3, 6, 12, 24, 48 and 72 h as seen in Fig. 4B. The *SERCA* in pufferfish spleen increased significantly at 3 h and 48 h post-infection. At the early time after challenge, the early up-regulation of SERCA may be mainly involved in the signaling pathways leading to apoptosis by pathogen, and the later increase may be contribute to the regulation of cytoplasmic free-Ca^{2+} [90]. In addition, the expression of *CD38* in pufferfish spleen increased at 48 h after challenge, which may be associated with the higher concentration of Ca^{2+}. Higher expression of *SERCA* would decrease the intracellular Ca^{2+} concentration and lower expression of *CD38* would reduce extracellular Ca^{2+} entering the cells [89,91]. These results were consistent with the findings we obtained by flow cytometry analysis in Fig. 4A. It may be because, after 12 h of challenge, enough calcium ions (Ca^{2+}) in the cytosol act as the second signal molecule to mediate the immune response and regulate related proteins to prevent damage. These results will provide light for further study the function of calcium signaling in immune system after infection with *A. hydrophila* in pufferfish.

5. Conclusion

The study provides novel insight into the molecular mechanisms that regulate the immune response to pathogen stress in pufferfish spleen. Our data could provide comprehensive interpretation and accurate measurement of genes and proteins expression changes in immune system. Further studies are needed to clarify the molecular function of target genes and proteins.

Acknowledgements

This project was supported by National Natural Science Foundation of China (31472302, 31172432), and Foundation of Administration of Ocean and Fisheries of Guangdong Province, China (A201701B04).

Appendix A. Supplementary data

Supplementary data to this article can be found online at https://doi.org/10.1016/j.fsi.2019.05.016.

References

[1] A.J. Lu, X.C. Hu, Y. Wang, A.H. Zhu, L.L. Shen, J. Tian, et al., Skin immune response in the zebrafish, *Danio rerio* (Hamilton), to *Aeromonas hydrophila* infection: a transcriptional profiling approach, J. Fish Dis. 38 (2) (2015) 137–150.
[2] C. Banerjee, R. Goswami, G. Verma, M. Datta, S. Mazumder, *Aeromonas hydrophila* induced head kidney macrophage apoptosis in *Clarias batrachus* involves the activation of calpain and is caspase-3 mediated, Dev. Comp. Immunol. 37 (3–4) (2012) 323–333.
[3] E. Abdy, M. Alishahi, M.R. Tabandeh, M. Ghorbanpoor, H. Jafari, Comparative effect of Freund's adjuvant and *Aloe vera* L. gel on the expression of TNF-α and IL-1β in vaccinated *Cyprinus carpio* L. with *Aeromonas hydrophila* C. bacterin, Aquacult. Res. 47 (8) (2016) 2543–2552.
[4] G. Di, H. Li, C. Zhang, Y. Zhao, C. Zhou, S. Naeem, et al., Label-free proteomic analysis of intestinal mucosa proteins in common carp (*Cyprinus carpio*) infected with *Aeromonas hydrophila*, Fish Shellfish Immunol. 66 (2017) 11–25.
[5] T.J. Abraham, A. Roy, R.B. Julinta, J. Singha, P.K. Patil, Efficacy of oxytetracycline and potentiated sulphonamide oral therapies against *Aeromonas hydrophila* infection in Nile tilapia *Oreochromis niloticus*, J. Coast. Life Med. (2017) 371–374.
[6] N.T. Tran, Z.X. Gao, H.H. Zhao, S.K. Yi, B.X. Chen, Y.H. Zhao, et al., Transcriptome analysis and microsatellite discovery in the blunt snout bream (*Megalobrama amblycephala*) after challenge with *Aeromonas hydrophila*, Fish Shellfish Immunol. 45 (1) (2015) 72–82.
[7] Y. Gong, S. Feng, S. Li, Y. Zhang, Z. Zhao, M. Hu, et al., Genome-wide characterization of Toll-like receptor gene family in common carp (*Cyprinus carpio*) and their involvement in host immune response to *Aeromonas hydrophila* infection, Comp. Biochem. Physiol. Genom. Proteonom. 24 (2017) 89–98.
[8] Y.F. Dang, Y.B. Shen, X.Y. Xu, S.T. Wang, X.Z. Meng, L.S. Li, et al., Mannan-binding lectin-associated serine protease-1 (MASP-1) mediates immune responses against *Aeromonas hydrophila in vitro* and *in vivo* in grass carp, Fish Shellfish Immunol. 66 (2017) 93–102.
[9] Z. Hu, B. Wu, F. Meng, Z. Zhou, H. Lu, H. Zhao, Impact of molecular hydrogen treatments on the innate immune activity and survival of zebrafish (*Danio rerio*) challenged with *Aeromonas hydrophila*, Fish Shellfish Immunol. 67 (2017) 554–560.
[10] X. Wen, L. Wang, W. Zhu, D. Wang, X. Li, X. Qian, et al., Three toll-like receptors (TLRs) respond to *Aeromonas hydrophila* or lipopolysaccharide challenge in pufferfish, Takifugu fasciatus, Aquaculture 481 (2017) 40–47.
[11] C.H. Cheng, S.W. Luo, C.X. Ye, A.L. Wang, Z.X. Guo, Identification, characterization and expression analysis of tumor suppressor protein p53 from pufferfish (*Takifugu obscurus*) after the *Vibrio alginolyticus* challenge, Fish Shellfish Immunol. 59 (2016) 312–322.
[12] Z. Qi, P. Wu, Q. Zhang, Y. Wei, Z. Wang, M. Qiu, et al., Transcriptome analysis of soiny mullet (*Liza haematocheila*) spleen in response to *Streptococcus dysgalactiae*, Fish Shellfish Immunol. 49 (2016) 194–204.
[13] G. Li, Y. Zhao, Z. Liu, C. Gao, F. Yan, B. Liu, et al., De novo assembly and characterization of the spleen transcriptome of common carp (*Cyprinus carpio*) using Illumina paired-end sequencing, Fish Shellfish Immunol. 44 (2) (2015) 420–429.
[14] S.D. Hwang, J.S. Bae, D.H. Jo, K.I. Kim, M.Y. Cho, B.Y. Jee, et al., Gene expression and functional characterization of serum amyloid P component 2 in rock bream, *Oplegnathus fasciatus*, Fish Shellfish Immunol. 47 (1) (2015) 521–527.
[15] S. Grove, R. Johansen, L.J. Reitan, C.M. Press, B.H. Dannevig, Quantitative investigation of antigen and immune response in nervous and lymphoid tissues of Atlantic halibut (*Hippoglossus hippoglossus*) challenged with nodavirus, Fish Shellfish Immunol. 21 (5) (2006) 525–539.
[16] Y. Mu, F. Ding, P. Cui, J. Ao, S. Hu, X. Chen, Transcriptome and expression profiling analysis revealed changes of multiple signaling pathways involved in immunity in the large yellow croaker during *Aeromonas hydrophila* infection, BMC Genomics 11 (2010).
[17] S. Li, Y. Zhang, Y. Cao, D. Wang, H. Liu, T. Lu, Trancriptome profiles of Amur sturgeon spleen in response to *Yersinia ruckeri* infection, Fish Shellfish Immunol. 70 (2017) 451–460.
[18] Y. Yang, H. Yu, H. Li, A. Wang, H.Y. Yu, Effect of high temperature on immune response of grass carp (*Ctenopharyngodon idellus*) by transcriptome analysis, Fish Shellfish Immunol. 58 (2016) 89–95.
[19] J.C. Vera, C.W. Wheat, H.W. Fescemyer, M.J. Frilander, D.L. Crawford, I. Hanski, et al., Rapid transcriptome characterization for a nonmodel organism using 454 pyrosequencing, Mol. Ecol. 17 (7) (2008) 1636–1647.
[20] N.L. Anderson, N.G. Anderson, Proteome and proteomics: new technologies, new concepts, and new words, Electrophoresis 19 (11) (1998) 1853–1861.
[21] W.K. Tse, J. Sun, H. Zhang, A.Y. Law, B.H. Yeung, S.C. Chow, et al., Transcriptomic and iTRAQ proteomic approaches reveal novel short-term hyperosmotic stress responsive proteins in the gill of the Japanese eel (*Anguilla japonica*), J. Proteomics 89 (2013) 81–94.
[22] L. Wang, C. Shao, W. Xu, Q. Zhou, N. Wang, S. Chen, Proteome profiling reveals immune responses in Japanese flounder (*Paralichthys olivaceus*) infected with Edwardsiella tarda by iTRAQ analysis, Fish Shellfish Immunol. 66 (2017) 325–333.
[23] X. Ren, X. Yu, B. Gao, J. Li, P. Liu, iTRAQ-based identification of differentially expressed proteins related to growth in the swimming crab, *Portunus trituberculatus*, Aquacult. Res. 48 (6) (2017) 3257–3267.
[24] M. Naderi, S. Keyvanshokooh, A.P. Salati, A. Ghaedi, Proteomic analysis of liver tissue from rainbow trout (*Oncorhynchus mykiss*) under high rearing density after administration of dietary vitamin E and selenium nanoparticles, Comp. Biochem. Physiol. Genom. Proteonom. 22 (2017) 10–19.
[25] E.M. Yu, H.F. Zhang, Z.F. Li, G.J. Wang, H.K. Wu, J. Xie, et al., Proteomic signature of muscle fibre hyperplasia in response to faba bean intake in grass carp, Sci. Rep. 7 (2017) 45950.
[26] P.F. Liu, Y. Du, L. Meng, X. Li, Y. Liu, Proteomic analysis in kidneys of Atlantic salmon infected with *Aeromonas salmonicida* by iTRAQ, Dev. Comp. Immunol. 72 (2017) 140–153.
[27] A. Mahanty, G.K. Purohit, S. Banerjee, D. Karunakaran, S. Mohanty, B.P. Mohanty, Proteomic changes in the liver of *Channa striatus* in response to high temperature stress, Electrophoresis 37 (12) (2016) 1704–1717.
[28] Z. Yang, Y. Chen, Length-weight relationship of obscure puffer (*Takifugu obscurus*) during spawning migration in the Yangtze river, China, J. Freshw. Ecol. 18 (3) (2003) 349–352.
[29] J. Wang, H. Tang, X. Zhang, X. Xue, X. Zhu, Y. Chen, et al., Mitigation of nitrite toxicity by increased salinity is associated with multiple physiological responses: a case study using an economically important model species, the juvenile obscure puffer (*Takifugu obscurus*), Environ. Poll. 232 (2018) 137–145.
[30] C.H. Cheng, C.X. Ye, Z.X. Guo, A. L, Wang, Immune and physiological responses of pufferfish (*Takifugu obscurus*) under cold stress, Fish Shellfish Immunol. 64 (2017) 137–145.
[31] W.S. Kim, J.M. Kim, S.K. Yi, H.T. Huh, Endogenous circadian rhythm in the river puffer fish *Takifugu obscurus*, Mar. Ecol. Prog. Ser. 153 (1997) 293–298.
[32] S. Fu, M. Ding, Y. Yang, J. Kong, Y. Li, Z. Guo, et al., Molecular cloning, characterization and expression analysis of caspase-6 in puffer fish (*Takifugu obscurus*), Aquaculture 490 (2018) 311–320.
[33] C.H. Cheng, F.F. Yang, S.A. Liao, Y.T. Miao, C.X. Ye, A.L. Wang, et al., Identification, characterization and functional analysis of anti-apoptotic protein BCL-2-like gene from pufferfish, *Takifugu obscurus*, responding to bacterial challenge, Fish Physiol. Biochem. 41 (4) (2015) 1053–1064.
[34] R. Geng, Y. Jia, M. Chi, Z. Wang, H. Liu, W. Wang, RNase1 alleviates the *Aeromonas hydrophila*-induced oxidative stress in blunt snout bream, Dev. Comp. Immunol. 91 (2019) 8–16.
[35] X. Du, Y. Li, D. Li, F. Lian, S. Yang, J. Wu, et al., Transcriptome profiling of spleen provides insights into the antiviral mechanism in *Schizothorax prenanti* after poly (I : C) challenge, Fish Shellfish Immunol. 62 (2017) 13–23.
[36] Y. Li, J. Wu, D. Li, A. Huang, G. Bu, F. Meng, et al., Transcriptome analysis of spleen reveals the signal transduction of toll-like receptors after *Aeromonas hydrophila* infection in *Schizothorax prenanti*, Fish Shellfish Immunol. 84 (2019) 816–824.
[37] B. Li, C.N. Dewey, RSEM: accurate transcript quantification from RNA-Seq data with or without a reference genome, BMC Bioinf. 12 (2011).
[38] C. Trapnell, B.A. Williams, G. Pertea, A. Mortazavi, G. Kwan, M.J. van Baren, et al., Transcript assembly and quantification by RNA-Seq reveals unannotated transcripts and isoform switching during cell differentiation, Nat. Biotechnol. 28 (5) (2010) 511-U174.
[39] S. Anders, W. Huber, Differential expression analysis for sequence count data, Genome Biol. 11 (10) (2010).
[40] Y. Benjamini, Y. Hochberg, Controlling the false discovery rate-a practical and powerful approach to multiple testing, J. R. Stat. Soc. B 57 (1) (1995) 289–300.
[41] Y. Yang, H. Yu, H. Li, A. Wang, Transcriptome profiling of grass carp (*Ctenopharyngodon idellus*) infected with *Aeromonas hydrophila*, Fish Shellfish Immunol. 51 (2016) 329–336.
[42] Y. Yang, H. Yu, H. Li, A. Wang, H. y. Yu, Effect of high temperature on immune response of grass carp (*Ctenopharyngodon idellus*) by transcriptome analysis, Fish Shellfish Immunol. 58 (2016) 89–95.
[43] Q. Shi, L.N. Chen, B.Y. Zhang, K. Xiao, W. Zhou, C. Chen, et al., Proteomics analyses for the global proteins in the brain tissues of different human prion diseases, Mol. Cell. Proteom. 14 (4) (2015) 854–869.
[44] E. Ferreira, D.M. Shaw, S. Oddo, Identification of learning-induced changes in protein networks in the hippocampi of a mouse model of Alzheimer's disease, Transl. Psychiatry 6 (2016).
[45] M. Ding, M. Chen, X. Zhong, Y. Wang, S. Fu, X. Yin, et al., Identification and characterization of C1 inhibitor in Nile tilapia (*Oreochromis niloticus*) in response to pathogenic bacteria, Fish Shellfish Immunol. 61 (2017) 152–162.
[46] K.J. Livak, T. D, Schmittgen. Analysis of relative gene expression data using real-time quantitative PCR and the 2(T)(-Delta Delta C) method, Methods 25 (4) (2001) 402–408.
[47] J.A. Xian, A.L. Wang, C.X. Ye, X.D. Chen, W.N. Wang, Phagocytic activity, respiratory burst, cytoplasmic free-Ca(2+) concentration and apoptotic cell ratio of haemocytes from the black tiger shrimp, *Penaeus monodon* under acute copper stress, Comp. Biochem. Physiol. C Toxicol. Pharmacol. 152 (2) (2010) 182–188.
[48] L. Tort, Stress and immune modulation in fish, Dev. Comp. Immunol. 35 (12) (2011) 1366–1375.
[49] A.E. Ellis, Innate host defense mechanisms of fish against viruses and bacteria, Dev. Comp. Immunol. 25 (8–9) (2001) 827–839.
[50] M. Bansal, A. Califano, Genome-wide dissection of posttranscriptional and

posttranslational interactions, in: B. Deplancke, N. Gheldof (Eds.), Gene Regulatory Networks: Methods and Protocols, 2012, pp. 131–149.
[51] A.R. Poh, R.J.J. O' Donoghue, M. Ernst, Hematopoietic cell kinase (HCK) as a therapeutic target in immune and cancer cells, Oncotarget 6 (18) (2015) 15752–15771.
[52] P.G. Chu, L.M. Weiss, Keratin expression in human tissues and neoplasms, Histopathology 40 (5) (2002) 403–439.
[53] F.A. Martin, R.P. Murphy, P.M. Cummins, Thrombomodulin and the vascular endothelium: insights into functional, regulatory, and therapeutic aspects, Am. J. Physiol. Heart C 304 (12) (2013) H1585–H1597.
[54] A. Bogdanovic, F. Bruckert, T. Morio, M. Satre, A syntaxin 7 homologue is present in *Dictyostelium discoideum* endosomes and controls their homotypic fusion, J. Biol. Chem. 275 (47) (2000) 36691–36697.
[55] Z. Herceg, Z.Q. Wang, Functions of poly(ADP-ribose) polymerase (PARP) in DNA repair, genomic integrity and cell death, Mutat. Res. Fund. Mol. M 477 (1–2) (2001) 97–110.
[56] J. Ee Uli, C.S.Y. Yong, S.K. Yeap, J.J. Rovie-Ryan, N. Mat Isa, S.G. Tan, et al., RNA sequencing (RNA-Seq) of lymph node, spleen, and thymus transcriptome from wild Peninsular Malaysian cynomolgus macaque (*Macaca fascicularis*), PeerJ 5 (2017) e3566.
[57] N.A. Ballesteros, R. Castro, B. Abos, S.S. Rodriguez Saint-Jean, S.I. Perez-Prieto, C. Tafalla, The pyloric caeca area is a major site for IgM(+) and IgT(+) B cell recruitment in response to oral vaccination in rainbow trout, PLoS One 8 (6) (2013).
[58] Z. Xu, F. Takizawa, D. Parra, D. Gomez, L. v. G. Jorgensen, S.E. LaPatra, et al., Mucosal immunoglobulins at respiratory surfaces mark an ancient association that predates the emergence of tetrapods, Nat. Commun. 7 (2016).
[59] U. Grimholt, MHC and evolution in teleosts, Biology 5 (1) (2016).
[60] W. Luo, J. Zhang, J.F. Wen, H. Liu, W.M. Wang, Z.X. Gao, Molecular cloning and expression analysis of major histocompatibility complex class I, IIA and IIB genes of blunt snout bream (*Megalobrama amblycephala*), Dev. Comp. Immunol. 42 (2) (2014) 169–173.
[61] C. Li, X. Wang, Q. Zhang, Z. Wang, J. Qi, Q. Yi, et al., Identification of two major histocompatibility (MH) class II A genes and their association to *Vibrio anguillarum* infection in half-smooth tongue sole (*Cynoglossus semilaevis*), J. O. U. China. 11 (1) (2012) 32–44 2012.
[62] Y.X. Zhang, S.L. Chen, Molecular identification, polymorphism, and expression analysis of major histocompatibility complex class IIA and B genes of turbot (*Scophthalmus maximus*), Mar. Biotechnol. 8 (6) (2006) 611–623.
[63] M.A. Kerr, The structure and function of human IgA, Biochem. J. 271 (2) (1990) 285–296.
[64] J. Ye, I.M. Kaattari, C. Ma, S. Kaattari, The teleost humoral immune response, Fish Shellfish Immunol. 35 (6) (2013) 1719–1728.
[65] J.D. Hansen, E.D. Landis, R.B. Phillips, Discovery of a unique Ig heavy-chain isotype (IgT) in rainbow trout: implications for a distinctive B cell developmental pathway in teleost fish, Proc. Natl. Acad. Sci. U.S.A. 102 (19) (2005) 6919–6924.
[66] N. Danilova, J. Bussmann, K. Jekosch, L.A. Steiner, The immunoglobulin heavy-chain locus in zebrafish: identification and expression of a previously unknown isotype, immunoglobulin Z, Nat. Immunol. 6 (3) (2005) 295–302.
[67] D. Gómez, J. Bartholomew, J.O. Sunyer, Biology and mucosal immunity to myxozoans, Dev. Comp. Immunol. 43 (2) (2014) 243–256.
[68] Y. Du, X. Tang, W. Zhan, J. Xing, X. Sheng, Immunoglobulin Tau heavy chain (IgT) in flounder, *Paralichthys olivaceus*: molecular cloning, characterization, and expression analyses, Int. J. Mol. Sci. 17 (9) (2016).
[69] I. Salinas, Y.A. Zhang, J.O. Sunyer, Mucosal immunoglobulins and B cells of teleost fish, Dev. Comp. Immunol. 35 (12) (2011) 1346–1365.
[70] R. Castro, L. Jouneau, H.P. Pham, O. Bouchez, V. Giudicelli, M.P. Lefranc, et al., Teleost fish mount complex clonal IgM and IgT responses in spleen upon systemic viral infection, Fish Shellfish Immunol. 34 (6) (2013) 1643–+.
[71] Y.A. Zhang, I. Salinas, J.O. Sunyer, Recent findings on the structure and function of teleost IgT, Fish Shellfish Immunol. 31 (5) (2011) 627–634.
[72] M. Oh hora, Calcium signaling in the development and function of T-lineage cells, Immunol. Rev. 231 (1) (2009) 210–224.
[73] S. Feske, Calcium signalling in lymphocyte activation and disease, Nat. Rev. Immunol. 7 (9) (2007) 690–702.
[74] B. Papp, J.P. Brouland, A. Arbabian, P. Gelebart, T. Kovacs, R. Bobe, et al., Endoplasmic reticulum calcium pumps and cancer cell differentiation, Biomolecules 2 (1) (2012) 165–186.
[75] E.R. Higgins, M.B. Cannell, J. Sneyd, A buffering SERCA pump in models of calcium dynamics, Biophys. J. 91 (1) (2006) 151–163.
[76] C.M. Freisinger, I. Schneider, T.A. Westfall, D.C. Slusarski, Calcium dynamics integrated into signalling pathways that influence vertebrate axial patterning, Philos. T. R. SOC. B 363 (1495) (2008) 1377–1385.
[77] D.E. Clapham, Calcium signaling, Cell 131 (6) (2007) 1047–1058.
[78] J.A. Dickinson, K.E. Hanrott, M.H. Mok, J.N. Kew, S. Wonnacott, Differential coupling of alpha7 and non-alpha7 nicotinic acetylcholine receptors to calcium-induced calcium release and voltage-operated calcium channels in PC12 cells, J. Neurochem. 100 (4) (2007) 1089–1096.
[79] J.A. Peterson, R.V. Oblad, J.C. Mecham, J.D. Kenealey, Resveratrol inhibits plasma membrane Ca^{2+}-ATPase inducing an increase in cytoplasmic calcium, Biochem. Biophys. Rep. 7 (2016) 253–258.
[80] M.A. Gillentine, J. Yin, A. Bajic, P. Zhang, S. Cummock, J.J. Kim, et al., Functional consequences of CHRNA7 copy-number alterations in induced pluripotent stem cells and neural progenitor cells, Am. J. Hum. Genet. 101 (6) (2017) 874–887.
[81] D. Oceandy, P.J. Stanley, E.J. Cartwright, L. Neyses, The regulatory function of plasma-membrane Ca^{2+}-ATPase (PMCA) in the heart, Biochem. Soc. Trans. 35 (2007) 927–930.
[82] C.H. Lin, W.C. Kuan, B.K. Liao, A.N. Deng, D.Y. Tseng, P.P. Hwang, Environmental and cortisol-mediated control of Ca(2+) uptake in tilapia (*Oreochromis mossambicus*), J. Comp. Physiol. B 186 (3) (2016) 323-232.
[83] B.K. Liao, A.N. Deng, S.C. Chen, M.Y. Chou, P.P. Hwang, Expression and water calcium dependence of calcium transporter isoforms in zebrafish gill mitochondrion-rich cells, BMC Genomics 8 (2007) 354.
[84] N. Chi Huu, S. Brenner, N. Huttary, Y. Li, A.G. Atanasov, V.M. Dirsch, et al., 12(S)-HETE increases intracellular Ca^{2+} in lymph-endothelial cells disrupting their barrier function in vitro; stabilization by clinical drugs impairing calcium supply, Cancer Lett. 380 (1) (2016) 174–183.
[85] G.G. Ignotz, S.S. Suarez, Calcium/calmodulin and calmodulin kinase II stimulate hyperactivation in demembranated bovine sperm, Biol. Reprod. 73 (3) (2005) 519–526.
[86] A. Deucher, T. Efimova, R.L. Eckert, Calcium-dependent involucrin expression is inversely regulated by protein kinase C (PKC)alpha and PKC delta, J. Biol. Chem. 277 (19) (2002) 17032–17040.
[87] T. Mirzapoiazova, J. Moitra, L. Moreno-Vinasco, S. Sammani, J.R. Turner, E.T. Chiang, et al., Non-muscle myosin light chain kinase isoform is a viable molecular target in acute inflammatory lung injury, Am. J. Resp. Cell Mol. 44 (1) (2011) 40–52.
[88] G.Y. Jung, Y.J. Park, J.S. Han, Effects of HA released calcium ion on osteoblast differentiation, J. Mater. Sci. Mater. Med. 21 (5) (2010) 1649–1654.
[89] K. Mehta, U. Shahid, F. Malavasi, Human CD38, a cell-surface protein with multiple functions, FASEB J. 10 (12) (1996) 1408–1417.
[90] E.S. Dremina, V.S. Sharov, K. Kumar, A. Zaidi, E.K. Michaelis, C. Schoneich, Anti-apoptotic protein Bcl-2 interacts with and destabilizes the sarcoplasmic/endoplasmic reticulum Ca^{2+}-ATPase (SERCA), Biochem. J. 383 (2004) 361–370.
[91] M.E. Roegner, H.Y. Chen, R.D. Watson, Molecular cloning and characterization of a sarco/endoplasmic reticulum Ca^{2+} ATPase (SERCA) from Y-organs of the blue crab (*Callinectes sapidus*), Gene 673 (2018) 12–21.